INSTITUTE OF PHYSICS PUBLISHING JOURNAL OF PHYSICS D: APPLIED PHYSICS

J. Phys. D: Appl. Phys. **39** (2006) 4788–4798 doi:10.1088/0022-3727/39/22/009

Non-conservative electron transport in CF_4 in electric and magnetic fields crossed at arbitrary angles

S Dujko[1,2], R D White[1], K F Ness[1], Z Lj Petrović[2] and R E Robson[1]

[1] School of Mathematical and Physical Science, James Cook University, Townsville 4810, QLD, Australia

[2]Institute of Physics, University of Belgrade, PO Box 68, 11080 Zemun, Serbia

E-mail: Sasa.Dujko@jcu.edu.au

Received 3 August 2006, in final form 21 September 2006
Published 3 November 2006
Online at stacks.iop.org/JPhysD/39/4788

Abstract

A Monte Carlo simulation technique is used to investigate electron transport in carbon tetrafluoride (CF_4) for an arbitrary configuration of electric and magnetic fields. We investigate the way in which the transport coefficients and other swarm properties are influenced by the electric and magnetic field strengths and the angle between the fields. In addition, the sensitivity of transport data on the presence of non-conservative collisions (attachment/ionization) is analysed. It is found that the difference between the two sets of transport coefficients, *bulk* and *flux*, resulting from the explicit effects of non-conservative collisions, can be controlled either by the variation of the magnetic field strengths or by the angles between the fields. This study was initiated in order to obtain the transport data for input into the fluid models of magnetron and inductively coupled plasma discharges as well as several types of high energy particle detectors, and has resulted in a database of such transport data. Values and general trends in the profiles of mean energy, collision frequency, rate coefficients, drift velocity elements and diffusion tensor are reported here.

1. Introduction

Studies of transport processes of charged particle swarms in neutral gases under the influence of electric and magnetic fields crossed at arbitrary angles to each other is of interest both as a problem in basic physics and for applications in many areas. In plasma processing technology, the transport coefficients and properties of charged particle swarms in electric and magnetic fields are necessary input data for models of plasma reactors that involve magnetic fields. Modelling of a magnetron discharge can greatly benefit from these studies. There have been numerous studies of magnetron discharges (see, e.g., [1, 2] and references therein) but the recent two-dimensional hybrid model is of particular note [3, 4]. In this hybrid model, the low-energy electrons and ions in the collision-dominated bulk plasma region are treated using a fluid model while the fast, non-equilibrium electrons in the cathode region are treated by a Monte Carlo simulation. The fluid part is based on the local field approximation and requires the tabulation of electron transport coefficients as a function of the reduced fields E/n_0, B/n_0 and the angle ψ between the fields, where n_0 is the neutral number density. Apart from the modelling of a magnetron discharge, an understanding of the dependence of the electron transport coefficients on the angle between the electric and magnetic fields is vitally important. A recently developed two-dimensional, time-dependent model for the collision-dominated ICP, based on the relaxation continuum (RCT) theory, employs scaled dc electron transport coefficients in electric and magnetic fields [5]. These scaled dc transport data include the drift velocity and diffusion coefficient. For arbitrary field directions, the drift velocity components are derived in terms of drift velocity components for the parallel and orthogonal fields while the diffusion is assumed to be isotropic and estimated from the momentum

balance of electrons. Clearly, further advancements of such and similar models are directly dependent on accurate modelling of charged particles transport. Recent attempts to include accurate treatments of the effects of a magnetic field into plasma models have led to a better understanding of the power transfer to ICPs [6, 7]. For example, it was shown that inclusion of the $\boldsymbol{E} \times \boldsymbol{B}$ drift may lead to additional heating of ICPs [8, 9].

In contrast to fluid models and fluid parts of hybrid models, the kinetic components of hybrid plasma modelling require sets of good and reliable cross sections. The determination of low-energy electron–molecule cross sections from an inversion of swarm transport data is a well-established procedure [10–12]. According to this procedure, the cross sections are adjusted until some preset agreement is obtained between experimentally and theoretically calculated transport coefficients. The application of an orthogonal configuration of electric and magnetic fields gives rise to an additional number of transport coefficients and thus one is able to exploit this in the inversion procedure. Thus by varying the magnitude of a magnetic field an additional check on the validity of a cross section set may be made through electron swarm data. For an arbitrary configuration of electric and magnetic fields, the degrees of freedom are further increased by varying the angle between the fields. In such cases the number of independent transport coefficients is even greater.

In addition to plasma processing technology, the transport of charged particle swarms under the action of electric and magnetic fields is a key subject for the optimization and design of radiation and high-energy elementary particle detectors [13]. These detectors are usually operated under various configurations of electric and magnetic fields with specific requirements on the transport properties of the swarm needed to achieve the desired spatial and temporal resolution for detection, big and fast signals, good energy deposition per unit length, etc. In any case, the inclusion of a magnetic field is necessary for particle momentum measurement [14]. Apart from the studies of electron transport in spatially uniform fields, recent studies of the ionization coefficient in a non-uniform electric field [15] and other transport data in slightly inhomogeneous fields [16] have attracted considerable attention.

Studies of electron transport in spatially homogeneous electric and magnetic fields have been the subject of interest for a number of years. The relaxation of electrons in electric and magnetic fields at arbitrary angles has been studied using the two-term approximation for solving the Boltzmann equation [17]. In order to overcome the limitations of the two-term approximation a general formalism for solving the Boltzmann equation for reacting charged-particles swarms in neutral gases was developed [18] and the numerical solution was applied to a range of gases with conservative and non-conservative processes for an orthogonal field configuration [19–22]. A non-trivial extension of the theory and associated code to include the arbitrary field configuration was developed and applied to a series of conservative model gases [23] and recently for the modelling of a magnetron oxygen discharge [24]. Other theoretical and numerical methods have also been applied to this problem. These include the semi-quantitative momentum transfer theory [25] and Monte Carlo simulation [26, 27]. The large and diverse literature associated with this type of problem has already been reviewed in [28] and will not be repeated here.

In this paper we present the first systematic treatment of non-conservative, spatially inhomogeneous electron swarms in electric and magnetic fields crossed at arbitrary angles for carbon tetrafluoride (CF_4) using a Monte Carlo simulation technique. CF_4 provides an example of a gas which has applications in a wide range of devices where the electron kinetics plays an important role in device behaviour. These applications include various types of radiation detectors [29, 30], gas discharge opening switches [31] and gaseous dielectrics [32]. CF_4 also has application in RF plasmas mostly realized in capacitively coupled plasma (CCP) [33] and even in ICP [34] for silicon etching. The knowledge of electron transport coefficients and in particular the values of electric and magnetic field strengths for which non-conservative collisions (attachment/ionization) may or may not have a significant effect on the drift and diffusion properties may be important for the operation of these devices. In this work, the transport coefficients are presented as a function of E/n_0, B/n_0 and the angle ψ appropriate to modelling the plasma reactors and for the optimization of radiation detectors.

In section 2, we give a brief discussion of the Monte Carlo method under non-conservative conditions for arbitrary angles between electric and magnetic fields. In section 3, we present results of a systematic study of electron transport in CF_4. This work may be viewed as an extension of the recently published papers of Biagi [26] and Dujko *et al* [27] for an orthogonal field configuration. We try to complement these previous publications by a comprehensive description of electron transport for the most general case of arbitrary field directions. In addition, in this paper we make a further generalization with respect to the work of White *et al* [24] to consider the explicit non-conservative effects. Finally, CF_4 is well known for producing negative differential conductivity (NDC) and in this work we demonstrate the variation of the drift speed with electric and magnetic field strengths and angle between the fields.

2. Monte Carlo procedure, quantities calculated

2.1. Outline of procedure

The Monte Carlo simulation technique used for an orthogonal configuration of electric and magnetic fields is discussed in our previous paper [27]. Rather than present a full review of the simulation technique, we highlight below some important points associated with the technique and differences due to the extension of our code to include the magnetic field at an arbitrary angle to the electric field.

The inclusion of an arbitrarily oriented magnetic field with respect to the electric field vector introduces some additional complexity in the electron motion. In such a case, the application of Boris rotation algorithm widely used for numerical integration of the equation of electron movement for an orthogonal field configuration may not be of much use and has to be replaced by an analytical solution. We employ the coordinate system where the electric field $\boldsymbol{E}$ defines the z-axis, while the magnetic field $\boldsymbol{B}$ lies in the y–z plane, making

an angle ψ with respect to the electric field $\boldsymbol{E}$. Hence, the equations of electron motion can be given analytically and the reader is referred to [26] for an explicit form of these equations.

The only unknown is the time step for the determination of the exact moment of the next collision. This is determined by solving the equation for the collision probability, using either the null-collision [35] or integration technique [36]. In our code, the latter approach is employed. All dynamic properties of each electron such as the position, velocity and energy can be updated and the electron motion through the neutral gas can be followed between collisions.

The angular distributions of both elastic and inelastic collisions are taken to be isotropic. It must be emphasized that this approximation is generally valid for relatively low E/n_0 but needs to be corrected when forward scattering becomes dominant. In that respect, Biagi has adopted the method proposed by Longo and Capitelli [37] in his Monte Carlo code to include the angular distribution of both elastic and inelastic collisions [26]. For CF_4, it was shown by Vasenkov [38] that the errors in transport coefficients, resulting from the assumption of isotropic scattering are less than about 3% for E/n_0 below 0.1 Td. For higher E/n_0, the errors increase rapidly up to 35%. In addition, it is necessary to re-consider the influence of superelastic collisions in an effort to account properly for the behaviour of electron swarms at low energies. However, since we attempt to scan a wide range of transport coefficients and to provide a database for plasma modelling, we will not focus on these issues in the present paper. In this context, it is the synergism of magnetic fields and non-conservative collisions in electron transport upon which we focus our attention.

2.2. Transport coefficients, definitions and calculation

Transport coefficients up to and including diffusion after relaxation to the steady state are determined from [39–41]. The number changing reaction rate is defined by

$$\alpha = -\frac{\mathrm{d}}{\mathrm{d}t}(\ln N), \tag{1}$$

the bulk drift velocity by

$$\boldsymbol{W} = \frac{\mathrm{d}}{\mathrm{d}t}\langle r\rangle, \tag{2}$$

and the bulk diffusion tensor by

$$\boldsymbol{D} = \frac{1}{2!}\frac{\mathrm{d}}{\mathrm{d}t}\langle \boldsymbol{r}^*\boldsymbol{r}^*\rangle, \tag{3}$$

where N is the total number of electrons at any time and $\boldsymbol{r}^* = \boldsymbol{r} - \langle \boldsymbol{r}\rangle$. These so-called 'bulk' or real space transport coefficients may be determined from the mean position of the electron swarm in configuration space [42]. In the absence of non-conservative collisions, one may avoid the differentiation required to obtain the drift velocity and components of the diffusion tensor by using the so-called 'flux' quantities. Hence the flux drift velocity components and the flux diagonal elements of the diffusion tensor are given by

$$W_i = \left\langle \frac{\mathrm{d}r_i}{\mathrm{d}t}\right\rangle = \langle v_i\rangle, \tag{4}$$

$$D_{ii} = \langle r_i v_i\rangle - \langle r_i\rangle\langle v_i\rangle, \tag{5}$$

where v_i is the electron velocity and $i = x, y, z$. It follows from (2) that the bulk drift velocity is the displacement of the mean position of the electron swarm and it describes the motion of the centre of mass of the total ensemble of electrons. On the other hand, the flux drift velocity is the mean velocity of the electrons. These two sets of transport coefficients are equal, by the definition, in the absence of non-conservative collisions (ionization/attachment); however in the presence of non-conservative processes they may differ. The distinction between these two sets of transport coefficients was discussed at length in the 1980s [43], but has been ignored in the majority of previous work in the plasma modelling community. This has lead to a potentially serious mismatch between input swarm data (generally the bulk transport properties) and the parameters (often the flux transport properties) required in many plasma fluid models [44, 45]. Note that only theory, i.e. Boltzmann equation calculations and/or Monte Carlo simulations, can resolve any such mismatch, by providing *both* flux and bulk transport coefficients.

2.3. Tensor structure

Another important issue is the structure of vector and tensor transport coefficients for an arbitrary field orientation. In contrast to the case of parallel ($\psi = 0$) or orthogonal ($\psi = 90^\circ$) electric and magnetic fields, where the tensors are sparse and symmetries exist among the elements, the general field configuration has all full vectors and tensors. Thus, for example, for arbitrary ψ (with $\boldsymbol{E}$ along a principal axis) there are three independent components of the drift velocity and nine independent components of the diffusion tensor. In the magnetic field free case, the diagonal elements of the diffusion tensor can differ sometimes by a factor of 6 [46] and this is further enhanced when a magnetic field is applied. Further, the calculations in model gases confirm that the off-diagonal components of the diffusion tensor can have magnitudes of equivalent orders to those of the diagonal elements [45]. The lesson from this is that in any given case, one should at least estimate the relative magnitudes of the elements before simplifying for fluid modelling purposes. The common practice in plasma modelling of assuming isotropic diffusion, in which off-diagonal diffusion tensor components are neglected and diagonal elements assumed equal is clearly problematic, even in the absence of a magnetic field.

We approach the problem in two stages: initially, in this work, we focus on diagonal elements and defer the detailed consideration of the off-diagonal components of the diffusion tensor to a future paper.

3. Results and discussion

3.1. Details of the simulation conditions

The cross sections detailed in [47] were chosen for this study and are displayed in figure 1. CF_4 represents a

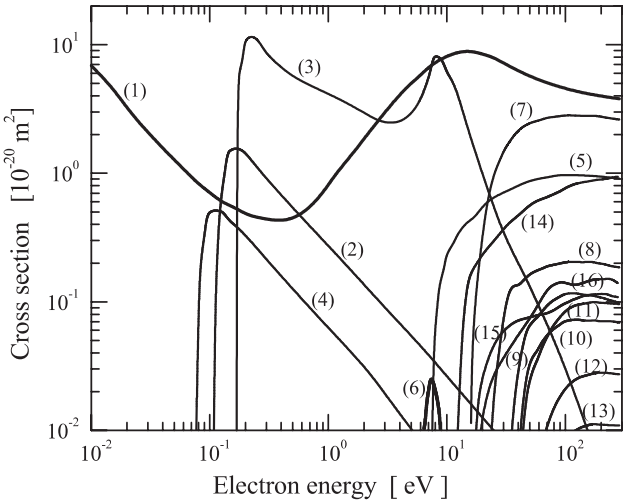

Figure 1. Electron impact cross-section for CF_4 used in this study [47] includes elastic momentum transfer (1), three vibrational (2–4) and one electronic excitation cross section (5), attachment cross section (6), seven dissociative ionization cross sections (7–13) and three cross sections for neutral dissociation (14–16).

molecular system with a deep Ramsauer–Townsend minimum in the elastic cross section. The two-term approximation, which is often employed for calculating electron transport parameters may fail for CF_4 due to a strong anisotropy of the velocity distribution function caused by the rapidly raising cross sections for vibrational excitation in the region of Ramsauer–Townsend minimum. The careful testing and systematic benchmarking of codes for calculations of transport properties is the critical step before they can be applied to model gas discharges. Our code was tested, among other things, using Reid's ramp model gas and model gases with non-conservative processes against a multi-term theory for solving the Boltzmann equation and found to be in good agreement [48].

We consider the reduced electric field range: 1–1000 Td (1 Td $= 10^{-21}$ V m^2), the reduced magnetic field range: 100–1000 Hx (1 Hx $= 10^{-27}$ T m^3) and the angles of 0°, 30°, 60° and 90° between the fields. The gas number density is 3.54×10^{22} m^{-3} which corresponds to the pressure of 1 Torr at 273 K. These simulation conditions overlap with the standard conditions found in plasma applications that involve magnetic fields.

3.2. Electron motion in electric and magnetic filed

Before embarking on a discussion of our results, we first look at the elementary description of electron motion in the electric and magnetic fields. The principal idea is to consider the effects of electron trajectories in order to explain certain trends in the profiles of the transport coefficients.

In the absence of collisions, electrons gyrate about the magnetic field lines at a frequency $\Omega = eB/m$ and with a Larmor radius $r = mc_T/eB$, where c_T is the tangential speed of the orbit. When collisions become important, it is convenient to break up the electron transport into three regions depending upon the relative strength of the magnetic field and the collisional processes. Firstly, there is a collision-dominated regime ($\Omega \ll \nu$, where ν is the total collision rate) where electrons may complete only a part of their orbits between successive collisions. Secondly, there is an intermediate regime ($\Omega \approx \nu$) where the motion of electrons is very complicated. Finally, there is a magnetic field-controlled regime ($\Omega \gg \nu$) where electrons on average complete many circular orbits per collision. Classification of these regimes can be made through the comparison between the total collision rate and cyclotron frequency. In figure 2 we compare the total collision rate and the cyclotron frequencies for various magnetic field strengths and angles between the fields. These three regimes are clearly evident in the data presented.

3.3. Electron transport coefficients

In our previous study [24] we considered the influence of E/n_0, B/n_0 and ψ on electron transport in O_2. The study unearthed some generic features which are again observed in CF_4. We highlight these features and focus on a unique aspect for CF_4 and the explicit effects of non-conservative collisions on transport coefficients.

3.3.1. Mean energy. Figure 3 shows the variation of the mean energy ε with E/n_0 for various B/n_0 and ψ. For the magnetic field free case ($B/n_0 = 0$), the cross section properties are reflected in the profile of the mean energy as the electric field increases. We observe three distinct regions of transport as E/n_0 increases. The first initial slow rise with E/n_0 is associated with the intensive energy losses due to vibrational excitation. The sharp rise in mean energies in the range 0.1–3 eV signifies that the influence of the vibrational excitation is reduced. The following slow rise indicates the progressive influence of new inelastic channels opening up such as electronic excitation and neutral and dissociative ionization in controlling the energy of the swarm.

The application of a magnetic field essentially shifts the $B/n_0 = 0$ mean energy profile and the corresponding structures to the right, towards higher E/n_0, meaning a higher electric field is required to achieve the same mean energy. This effect is more evident as the angle between the fields is increased. In general, the mean energy is a monotonically decreasing function of both B/n_0 (keeping E/n_0 and ψ fixed) and ψ (keeping E/n_0 and B/n_0 fixed). This is the well-known phenomenon of 'magnetic cooling' and it results from an inability of the electric field to efficiently pump the energy into the system [19] because the electrons change the direction of motion due to the magnetic field. This phenomenon is enhanced as the component of the magnetic field perpendicular to the electric field is increased. It is interesting to note that this phenomenon is independent of the gas considered and has been observed previously for all model and real [23] gases. Only recently has it been shown that for a very narrow range of conditions the mean energy may begin to rise with the magnetic field [22]. In contrast to recent studies of electron transport in oxygen [24] and argon [22], the anomalous reduction in mean energy with E/n_0 at fixed B/n_0 for $\psi = 90°$ has not been observed. This suggests that interplay between magnetic field cooling and inelastic/ionization cooling due to the nature of the cross sections does not promote this phenomenon in the energy region covered in this study.

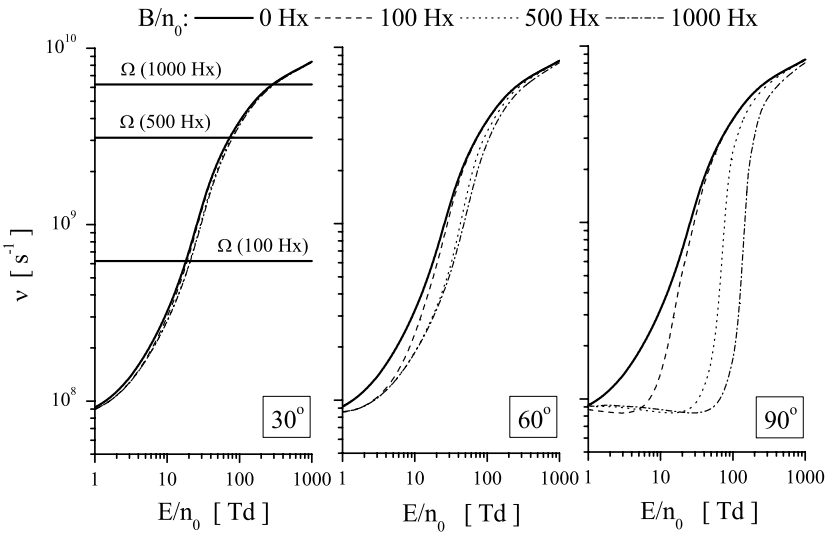

Figure 2. Comparison of the total collision rate and cyclotron frequencies as a function of E/n_0 for various B/n_0 and ψ.

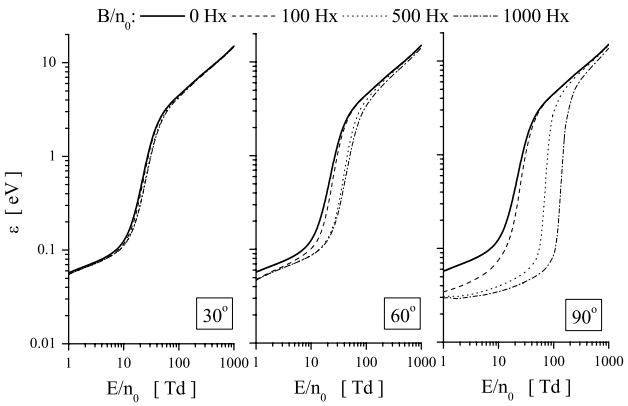

Figure 3. Variation of the mean energy as a function of E/n_0 for various B/n_0 and ψ.

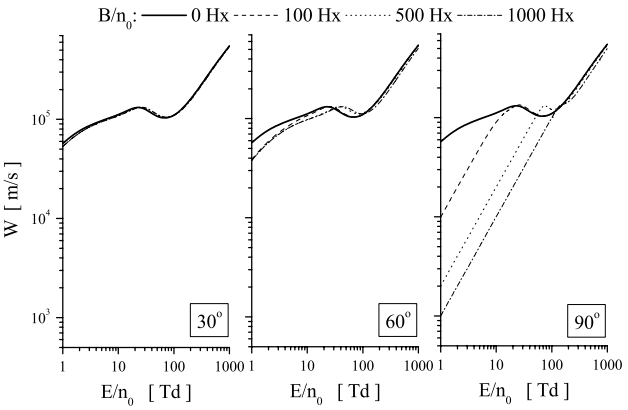

Figure 4. Variation of the drift speed as a function of E/n_0 for various B/n_0 and ψ.

3.3.2. Drift speed and drift velocity components. In this section we show the drift speed and drift velocity components as a function of E/n_0 for various B/n_0 and ψ. The drift speed shown in figure 4 exhibits a region of NDC, i.e. over a range of E/n_0 values the drift speed decreases as the driving field is increased. A comprehensive investigation of NDC for model gases in pure electric fields was performed by Petrović *et al* [49] and Robson [50]. As pointed out in these studies, NDC arises for certain *combinations* of elastic and inelastic cross sections in which, on increasing the electric field, there is a rapid transition in the dominant energy loss mechanism from inelastic to elastic. The determining factor is the how rapidly the *ratio* of the inelastic to elastic cross sections falls with the increasing mean energy/applied field. Typically, the effect is enhanced by either or both of (i) a rapidly increasing cross section for elastic collisions and (ii) a rapidly decreasing inelastic cross section. In the transition regime, the enhanced randomization of the directed motion decreases the drift velocity even though the mean energy increases. Once the conditions that promote NDC are set, then it is possible to induce and control it by: (i) non-conservative collisions [51], (ii) electron–electron collisions [52] and (iii) anisotropic scattering [53].

The combination of a rapidly increasing momentum transfer cross section for elastic collisions and a rapidly decreasing cross section for vibrational excitation in the region of the Ramsauer–Townsend minimum in CF_4 favours the development of NDC. It is interesting to note that this effect can be controlled either by varying the magnitude of a magnetic field or by the angle between the fields. The drift speed profiles shown in figure 4 display some interesting properties. The variation in drift speed with B/n_0 for small angles is relatively very small. However, as ψ increases, the position and depth of the NDC region are both changed. The drift speed profiles are shifted to the right towards higher E/n_0 values, while the depth of the NDC region is reduced. For orthogonal fields, NDC vanishes in the limit of high magnetic fields. In addition, we note the unusual variation of the drift speed associated with the variation of the angle ψ for certain fixed values of E/n_0. While ε monotonically decreases with increasing ψ for any fixed E/n_0 value, the drift speed may display a maximal property with ψ for certain fixed values of E/n_0. A similar behaviour of the drift speed was observed in methane [54].

One can understand the behaviour of drift speed and NDC in electric and magnetic fields through *an effective electric*

field [13]

$$E_{\text{eff}} = E\cos\phi, \tag{6}$$

where ϕ is the Lorentz angle (the angle between the drift velocity and the electric field). The displacement of the NDC region towards higher E/n_0 with increasing B/n_0 values then follows immediately from (6). Recent applications of the extended Tonk's theorem [27] confirm this observation. On the other hand, the reduction in and eventual vanishing of NDC in the limit of high magnetic fields for orthogonal fields cannot possibly be described by an effective electric field. This is perhaps evidence of additional variation of the velocity distribution function for both B/n_0 and ψ. One may use the same physical arguments to explain an increase in drift speed with the increasing magnetic field for certain values of E/n_0. As pointed out in [54], the application of a magnetic field leads to the Maxwellization of high-energy electrons while an increasing component of the magnetic field perpendicular to the electric field acts to decrease the anisotropy of the distribution function in velocity space in some specific planes. These two combined effects alter the ratio between the collision frequency for elastic and inelastic collisions in the energy region critical for development of NDC. These results clearly illustrate the limitations of the effective field concept in an attempt to model magnetized discharge and/or swarm experiments involving both electric and magnetic fields.

In figures 5–7 we show the drift velocity components as a function of E/n_0 for various B/n_0 and ψ. As can be seen, $W_x = W_y$ for $\psi = 0$ and $W_y = 0$ for $\psi = 90^\circ$. In particular, W_z shows the following interesting points (see figure 5). The W_z profiles at the smallest angle (covered here) overlap each other. As the angle between the fields increases there is a significant separation in the profiles. As a result, for the orthogonal field configuration W_z can vary over several orders of magnitude with B/n_0 and fixed E/n_0. However, this can be achieved only in the magnetic field-controlled regime. In the collision dominated regime the W_z profiles, as expected, become essentially independent of both B/n_0 and the angles between the fields.

In figure 6 we observe the following general features in the W_x profiles. In the magnetic field-controlled regime W_x is almost linear with E/n_0 indicating insensitivity to the details of the cross section in this regime. However, as E/n_0 increases, the W_x profiles depart from the linear regime and start to decrease, reaching the minimum, and then start to increase again. Also, in the magnetic field-dominated regime W_x is a monotonically decreasing function of B/n_0 while in the collision-dominated regime an opposite behaviour is clearly evident. One can explain this behaviour by considering electron orbits and the fact that an increasing magnetic field acts to reduce the mean energy and hence reduces the collisional impedance for the drift in that direction. Also, as can be seen, the W_x profiles have a weak sensitivity to the angle between the fields. As the angle between the fields increases the W_x profiles do not change significantly. Generally speaking, the behaviour of W_x results from a complex interplay between the explicit field effects and energy dependent collision frequency. It must be emphasized that previous investigations [24, 27] independently support the

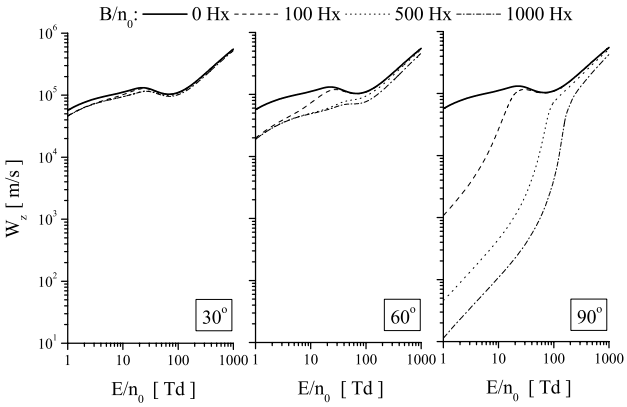

Figure 5. Variation of W_z as a function of E/n_0 for various B/n_0 and ψ.

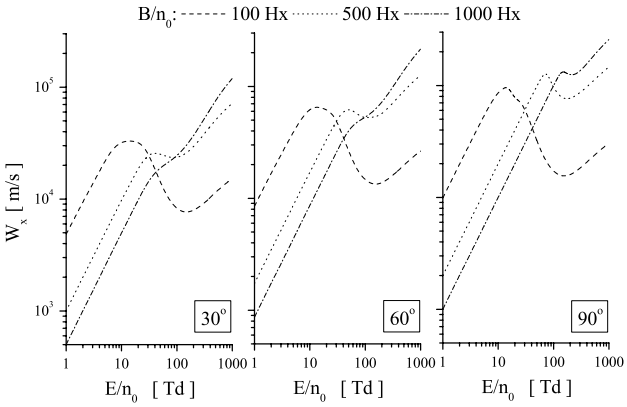

Figure 6. Variation of W_x as a function of E/n_0 for various B/n_0 and ψ.

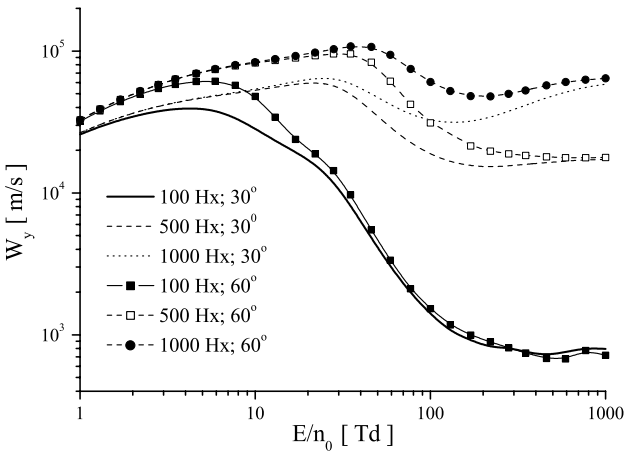

Figure 7. Variation of W_y as a function of E/n_0 for various B/n_0 and ψ.

general properties of this drift velocity component observed here indicating the predominant influence of the field effects.

The variation of W_y with E/n_0, B/n_0 and ψ is shown in figure 7. We show only the configuration for which W_y is non-zero. In the magnetic field-dominated regime the W_y profiles appear to be independent of B/n_0 and relatively dependent on ψ. As E/n_0 increases and the collisions start to play a significant role, one may observe that W_y becomes

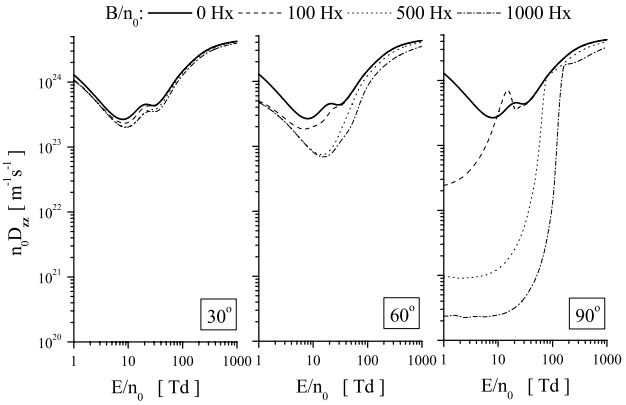

Figure 8. Variation of D_{zz} as a function of E/n_0 for various B/n_0 and ψ.

essentially independent of ψ and predominantly dependent on B/n_0 with W_y an increasing function of B/n_0. Another important property is that W_y shows a high sensitivity to the energy dependence of the cross sections [19]. It should be noted that a similar behaviour of this drift velocity component has been recently observed in oxygen [24].

3.3.3. Diagonal elements of diffusion tensor. In figures 8–10 we show the diagonal elements of the diffusion tensor as a function of E/n_0 for various B/n_0 and ψ. Due to the complexity and interplay of various factors which influence the diffusion tensor it is hard to fully understand and elucidate even the basic trends in the profiles of the diffusion tensor components. These factors include: (a) the thermal anisotropy effect resulting from the different random electron motions in different directions, (b) the magnetic anisotropy effect which acts to inhibit diffusion in the plane perpendicular to the magnetic field and (c) the electric anisotropy effect arising from a spatial variation of the average energy and local average velocities throughout the swarm which acts so as to either inhibit or enhance diffusion. In addition to this triple anisotropy effect, the effects of collisions, energy dependent total collision frequency and further couplings of these factors can further complicate the physical content of this issue. A convenient way to isolate and elucidate the phenomena associated only with the field effects is using a simple analytical form of cross sections in the calculations. The reader is referred to [23] for such discussion. In what follows we show the basic trends in the profiles of the diffusion tensor components and highlight interesting points where appropriate.

Figure 8 shows the variation of D_{zz} as a function of E/n_0 for various B/n_0 and ψ. The variation in D_{zz} with both E/n_0 and B/n_0 for the small angles between the fields is relatively very small. As ψ increases, in the magnetic field-controlled regime a significant difference between the profiles is established. As can be seen, D_{zz} monotonically decreases with ψ. For orthogonal fields D_{zz} may vary over five orders of magnitude with E/n_0 and B/n_0. However, as the profiles enter the collision-dominated regime, all the D_{zz} profiles approach the magnetic free profile, as expected.

The variation of D_{xx} with E/n_0, B/n_0 and ψ is shown in figure 9. In the magnetic field-controlled regime, D_{xx} decreases markedly with B/n_0. As ψ increases, keeping E/n_0 and B/n_0 fixed, D_{xx} is also a monotonically decreasing function. However, this reduction with ψ is not as apparent as that with B/n_0. Clearly, this indicates that the explicit orbital effect dominates the profiles in this regime. Finally, when the collision-dominated regime is achieved, all profiles approach the magnetic free profile. In summary, D_{xx} has limited sensitivity to the details of the cross section and again the field effects dominate the profiles.

In figure 10 we show the variation of D_{yy} as a function of E/n_0 for various B/n_0 and ψ. The most distinct property of D_{yy} is a high sensitivity to the energy dependence of the cross section. The richness of structures in the profile of D_{yy} makes this transport coefficient a good candidate for a fitting parameter in the prospective fine adjustment of cross sections. In the magnetic field-dominated regime, for a given B/n_0, D_{yy} monotonically increases with ψ indicating the reduction in the explicit orbital effect in the y-direction with increasing ψ. However, as E/n_0 increases, in the transition regime D_{yy} is dependent on both B/n_0 and ψ. Finally, in the collision-dominated regime all profiles approach the magnetic field free profile. In particular, it is interesting to consider the profiles of D_{yy} for orthogonal fields. Surprisingly for $\psi = 90^\circ$ in the magnetic field-dominated regime the values of D_{yy} for $B/n_0 \neq 0$ are greater than those for $B/n_0 = 0$. A similar phenomenon was observed in oxygen [24].

3.3.4. Rate coefficients. In figures 11 and 12 we show the attachment and ionization rate coefficients as a function of E/n_0 for various B/n_0 and ψ, respectively. The ionization rate coefficient increases with E/n_0 and monotonically decreases with both B/n_0 and ψ. The attachment rate has a similar dependence on B/n_0 and ψ. Its dependence on E/n_0, however, shows a maximum in the 100 Td region. This is intimately connected with the energy dependence of the cross sections and range of swarm mean energies. In the present study the swarm mean energy varies from the thermal value to about 20 eV. The relatively small attachment cross section has a sharp peak at around 7.5 eV. The ionization cross sections on the other hand still increase above this energy. Hence the variations of the attachment and ionization rates with E/n_0 follow.

3.3.5. The effects of non-conservative interactions on transport coefficients. In this section the influence of non-conservative collisions on electron transport is analysed by considering the difference between the bulk and flux values of a given transport coefficient. In figure 13 we show the percentage difference Δ between the bulk and flux values of the drift velocity components as a function of E/n_0 and various ψ where

$$\Delta = \frac{|\text{bulk}| - |\text{flux}|}{|\text{bulk}|} \cdot 100\%.$$

For illustrative purposes we chose B/n_0 of 1000 Hx to ensure a strong effect of the magnetic field on the transport coefficients. From figure 13 it is seen that attachment starts to affect the drift velocity components for E/n_0 greater than 40 Td. The value of E/n_0 for which this occurs, increases with ψ. In the range of 40–130 Td, where attachment is the dominant non-conservative process, the magnitudes of the flux values of

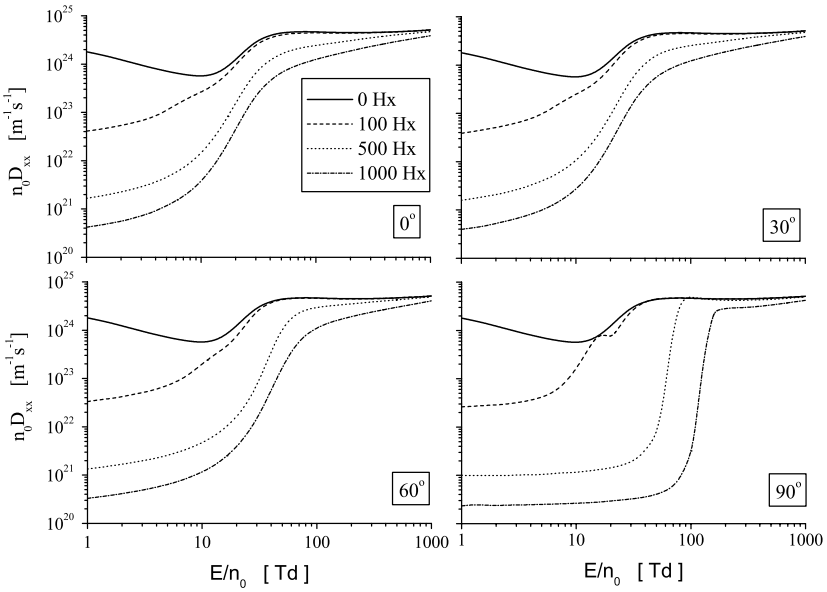

Figure 9. Variation of D_{xx} as a function of E/n_0 for various B/n_0 and ψ.

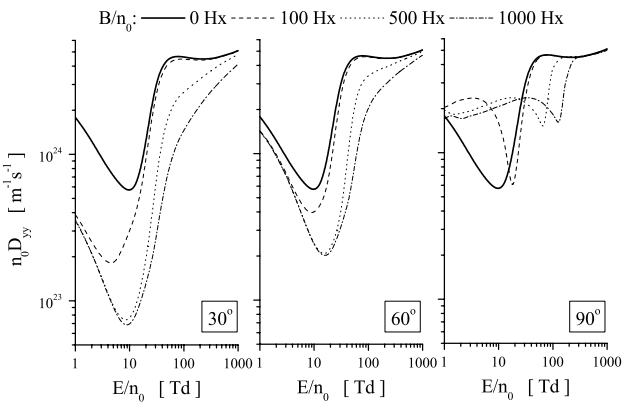

Figure 10. Variation of D_{yy} as a function of E/n_0 for various B/n_0 and ψ.

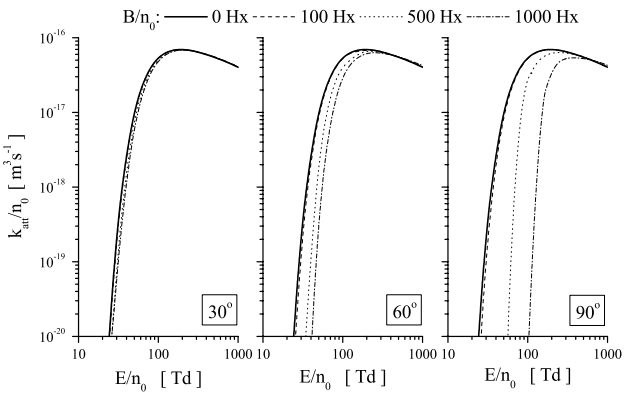

Figure 11. Variation of attachment rate coefficient k_{att} as a function of E/n_0 for various B/n_0 and ψ.

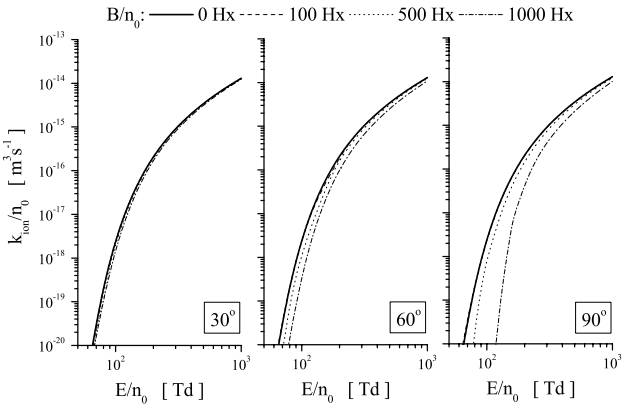

Figure 12. Variation of ionization rate coefficient k_{ion} as a function of E/n_0 for various B/n_0 and ψ.

W_z and W_y are greater than corresponding bulk values. The differences are less than approximately 2%. This effect is significantly reduced by the large inelastic processes in the vicinity of attachment (see figure 1). As E/n_0 increases, the influence of ionization becomes clearly evident. In the range of 130–1000 Td, the bulk magnitudes of W_z and W_y exceed the corresponding flux values. The rate coefficients for attachment and ionization cross each other in the same region, indicating that the production of free electrons by ionization dominates the loss of electrons through attachment. A further increase in E/n_0 leads to a more pronounced difference between the bulk and flux magnitudes of W_z and W_y, up to almost 30%. The differences between the bulk and flux magnitudes for W_z, however, are only slightly affected by the variation in ψ and one may observe the reduction in the differences between the bulk and flux values of W_y as ψ increases, particularly at higher E/n_0.

For the drift velocity component along the $\boldsymbol{E}\times\boldsymbol{B}$ direction, W_x appears to be less sensitive to the presence of non-conservative collisions. This is in agreement with previous works [23, 24, 27]. The non-conservative correction does not exceed about 5%. Further, and in contrast to W_z and W_y, in the range of 40–200 Td the magnitude of the bulk component of W_x is greater than its flux component. As E/n_0 increases above 200 Td, the difference between the bulk W_x and its flux

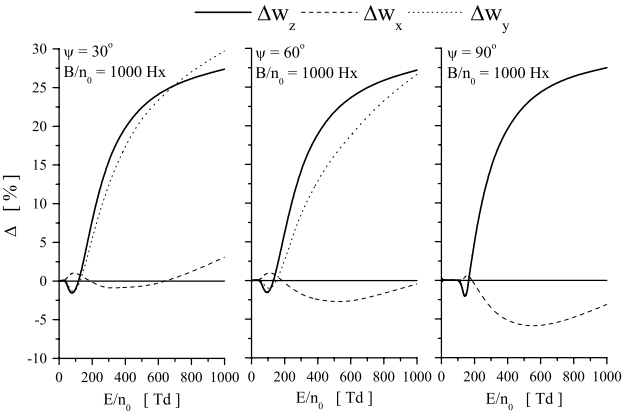

Figure 13. The percentage difference between the bulk and flux values of the drift velocity components as a function of E/n_0 for B/n_0 of 1000 Hx and ψ of 90°.

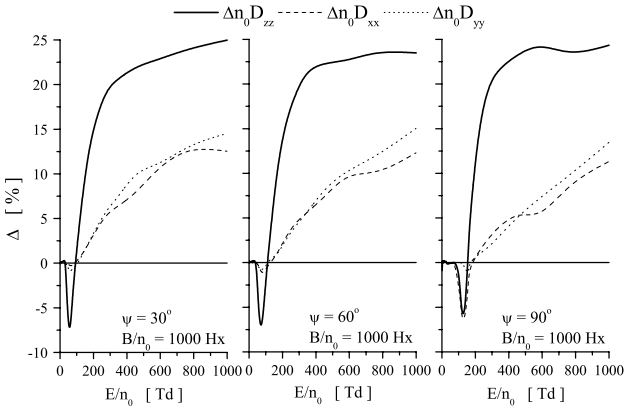

Figure 14. The percentage difference between the bulk and flux values of the diagonal elements of the diffusion tensor as a function of E/n_0 for B/n_0 of 1000 Hx and ψ of 90°.

component decreases, reaches the minimum and then starts to increase. From figure 13 it is seen that as ψ increases, the contribution of attachment becomes smaller while the ionization dominates in the non-conservative correction.

To understand the differences between bulk and flux transport we return to the origin of the difference between the two types of transport coefficients. The distinction between flux and bulk components of both drift velocity vector elements and diagonal elements of the diffusion tensor is a consequence of spatially dependent non-conservative collisions resulting from a spatial variation of average electron energies within the swarm [55]. If the attachment/ionization rate is an increasing function of electron energy, electrons are preferentially lost/created in regions of higher energy resulting in a shift in the centre of mass position as well as a modification of the spread about the centre of mass.

Consider the drift velocity in the $\boldsymbol{E}$ (z)-direction. The average energy always increases through the swarm in the direction of the electric force. Hence, at low E/n_0 ($E/n_0 <$ 130 Td) where attachment is the dominant non-conservative process, electrons are preferentially lost from the front of the swarm resulting in a shift of the centre of mass opposite in direction to the flux drift in that direction—the bulk magnitude is less than the flux magnitude in this region of E/n_0. The converse is true when ionization becomes the dominant non-conservative process ($E/n_0 >$ 130 Td). Electrons are preferentially created at the front of the swarm in the z-direction and hence the magnitude of the bulk drift component in this direction is greater than the equivalent flux component. The same physical picture applies for drift in the y-direction [23].

When we consider the drift velocity in the $\boldsymbol{E} \times \boldsymbol{B}$ direction, the picture is not as simple [22, 25]. The drift velocity component along the $\boldsymbol{E} \times \boldsymbol{B}$ direction, W_x, appears in general to be less sensitive to the effects of non-conservative collisions than the other components. This weak sensitivity of W_x to the non-conservative collisions is indicative of an essentially symmetric spatial profile (with a slight bias) of average energy about the centre of mass of the swarm in the $\boldsymbol{E} \times \boldsymbol{B}$ direction [23, 25]. Consequently, the essentially symmetric production/loss of electrons about the centre of mass by ionization/attachment processes do not have a major impact on the position of the centroid, and the small differences between bulk and flux components in this direction then follow. These small differences are due to the slight non-symmetrical bias in the spatial variation of the average energy in that direction. In contrast to both the y and z directions, where the average energy increases in the direction of the drift in these directions (independent of the electric field strength), in the x direction the spatial variation is dependent on the magnitude of the electric field. For low E/n_0 the average energy *decreases* in the direction of the drift. Hence, at fields where attachment is the dominant non-conservative process, the bulk is greater than the flux, while when ionization dominates the flux is greater than the bulk. At higher E/n_0 however, there is a transition to the normal situation where the average energy increases in the direction of the drift. This transition in the spatial variation of the average energy is evidenced by the second cross-over point in the profiles in figure 13. The regime where the bulk is greater than the flux is restored and is consistent with the other directions. This transition takes place at higher E/n_0 as ψ is increased.

To study in detail the non-conservative collisions effect on the diagonal elements of the diffusion tensor, a comprehensive investigation of spatially dependent mean energies and velocities through the swarm is inevitable. This is beyond the scope of this paper and the reader is referred to [25] where the simple analytical theory was used for certain model interaction cross sections. However, in this work we highlight some interesting points associated with the influence of non-conservative collisions on the diagonal elements of the diffusion tensor. In figure 14 we show the percentage difference between the bulk and flux values of the diagonal elements of the diffusion tensor as a function of E/n_0 and various ψ. The density-normalized magnetic field intensity is fixed at $B/n_0 =$ 1000 Hx. In the low E/n_0 range ($E/n_0 <$ 130 Td), where attachment is the dominant non-conservative process the differences between these two types of data can be greater than 5%. Having in mind the previous results for the drift velocity components, it follows that attachment affects the diffusion of the electrons more than it does the drift. For $\psi \neq 90°$ D_{zz} is the most sensitive component to the presence of attachment. For orthogonal fields, D_{zz} and D_{xx} show approximately equal sensitivity with respect to attachment.

As E/n_0 increases, the distinctions between the bulk and flux values of the diagonal elements of the diffusion tensor become more evident as the ionization rate increases. At the highest E/n_0 considered here these differences can be around 25%. This indicates that the increase in the electron number due to ionization enhances diffusion.

4. Conclusion

A comprehensive investigation of electron transport in CF_4 under the influence of electric and magnetic fields crossed at arbitrary angles to each other has been carried out. This investigation has resulted in a database of transport data which is applicable for a wide range of potential applications, although we focused upon the provision and correct implementation of swarm data within the fluid modelling of magnetron or ICP discharges.

Following previous works [24,27], the basic phenomenology of electron transport in electric and magnetic fields is presented on the basis of the ratio of the cyclotron to the collision frequencies. By doing so, the effects of a magnetic field on electron transport are separated from those generated by the collisions. The sensitivity of electron transport data to the energy dependence of the cross sections under the influence of electric and magnetic fields crossed at arbitrary angles to each other was considered. The drift velocity component and diffusion coefficient along the y-direction were identified as the most sensitive transport data to the energy dependence of the cross sections. We highlighted the potential use of these transport coefficients in the determination of low-energy electron–neutral cross sections.

In addition to the magnetic field strength, the variation of the angle between the fields on electron transport was considered. It was found that various transport coefficients show different sensitivities to the magnetic field strength and angle between the fields. In particular, the NDC associated with the drift speed may be controlled either by varying the magnitude of the magnetic field or by changing the angle between the fields. On the other hand, the $\boldsymbol{E} \times \boldsymbol{B}$ drift velocity component is almost insensitive to the angle between the fields. The drift velocity component along the y-direction is independent of B/n_0 and relatively dependent on ψ when a magnetic field controls the swarm behaviour. In the collision-dominated regime it appears independent of ψ and influenced only by B/n_0. Similar observations could be made for the diagonal elements of the diffusion tensor.

We have also considered the effect of non-conservative collisions on electron transport. These phenomena are associated with the spatial variation of the electron energy within the swarm resulting in spatially dependent non-conservative processes. It was shown that attachment has little effect on electron transport as can be expected from the weak electronegative nature of CF_4. On the other hand, above 130 Td ionization has a strong influence on electron transport and produces a visible distinction between the bulk and flux components of electron transport data. Various transport coefficients show different sensitivities to the presence of the non-conservative effects. The difference between the bulk and flux drift velocity components along electric field and y-direction are more sensitive to non-conservative collisions than the $\boldsymbol{E} \times \boldsymbol{B}$ component. A similar behaviour is observed for the diagonal elements of the diffusion tensor. The diffusion coefficient along the electric field is more sensitive to the non-conservative collisions than the other two components, indicating a higher order spatial dependence on average energy in this direction.

We have attempted to understand the non-conservative transport of electrons in CF_4 using a Monte Carlo method for calculations of both bulk and flux transport data. A warning to plasma fluid modelers who employ swarm data is: be aware of the differences between these two sets of transport coefficients! Any misunderstanding about the difference between these two or using one instead of the other may be the source of significant errors in plasma modelling [45]. The most appropriate procedure would be to use the experimental swarm data (e.g. bulk values) for the analysis of the validity of the cross section and then to calculate the flux quantities which are necessary as input data in fluid modelling of plasma discharges.

Acknowledgments

The authors would like to thank Dr Z M Raspopović and Professor Toshiaki Makabe for useful disscusions on issues associated with the topic of this paper. This work was supported by MNZZS Project 141025.

References

[1] Shon C H and Lee J K 2002 *Appl. Surf. Sci.* **192** 258
[2] Nanbu K, Mitsui K and Kondo S 2000 *J. Phys. D: Appl. Phys.* **33** 2274
[3] Shidoji E, Makabe T and Ness K F 2001 *Vacuum* **60** 299
[4] Shidoji E, Ohtake H, Nakano N and Makabe T 1999 *Japan. J.Appl. Phys.* **38** 2138
[5] Kamimura K, Iyanagi K, Nakano N and Makabe T 1999 *Japan. J. Appl .Phys.* **38** 4429
[6] Kinder R L and Kushner M 2001 *J. Appl. Phys.* **90** 3699
[7] Sankaran A and Kushner M 2002 *J. Appl. Phys.* **92** 736
[8] Tadokoro M, Hirata H, Nakano N, Petrović Z Lj and Makabe T 1998 *Phys. Rev.* E **57** R43–6
[9] Vasenkov A V and Kushner M J 2003 *J. Appl. Phys.* **94** 5522
[10] Crompton R W 1994 *Adv. At. Mol. Opt. Phys.* **32** 97
[11] Schmidt B 1993 *Comment. At. Mol. Phys.* **28** 379
[12] Schmidt B 1994 *Phys. Scr.* **T53** 30
[13] Robson R E, Hildebrandt M and Schmidt B 1997 *Nucl. Instrum. Methods* A **394** 74
[14] Blum W and Rolandi L, 1993 *Particle Detection with Drift Chambers* (Berlin: Springer)
[15] Mitev K, Segur P, Alkaa A, Bordage M C, Furstoss C, Khamphan C, de Nardo L, Conte V and Colautti P 2005 *Nucl. Instrum. Methods* A **538** 672
[16] Alcaraz J 2005 *Nucl. Instrum. Methods* A **553** 613
[17] Loffhagen D and Winkler R 1999 *IEEE Trans. Plasma Sci.* **27** 1262
[18] Ness K F 1993 *Phys Rev.* E **47** 327
[19] Ness K F 1994 *J. Phys. D: Appl. Phys.* **27** 1848
[20] Ness K F and Robson R E 1994 *Phys. Scr.* **T53** 5
[21] Ness K F 1995 *Aust. J. Phys.* **48** 557
[22] Ness K F and Makabe T 2000 *Phys. Rev. E* **62** 4083
[23] White R D, Ness K F, Robson R E and Li B 1999 *Phys. Rev.* E **60** 2231
[24] White R D, Ness K F, Robson R E and Makabe T 2005 *J. Phys. D: Appl. Phys.* **38** 997
[25] Li B, White R D, Robson R E and Ness K F 2001 *Ann. Phys.* **292** 179

[26] Biagi S F 1999 *Nucl. Instrum. Methods* A **421** 234
[27] Dujko S, Raspopović Z M and Petrović Z Lj 2005 *J. Phys. D: Appl. Phys.* **38** 2952
[28] White R D, Ness K F and Robson R E 2002 *Appl. Surf. Sci.* **192** 26
[29] Christophorou L G, Datskos P G and Carter J G 1991 *Nucl. Instrum. Methods* A **309** 160
[30] Razin V I 1995 *Nucl. Instrum. Methods* A **367** 295
[31] Hunter S R, Carter J G and Christophorou L G 1988 *Phys. Rev.* A **38** 58
[32] Pradazrol C, Casanovas A M, Hernoune A and Casanovas J 1996 *J. Phys. D: Appl. Phys.* **29** 1941
[33] Kitajima T, Takeo T, Petrović Z Lj and Makabe T 2000 *Appl. Phys. Lett.* **77** 489
[34] Hioki K, Hirata H, Nakano N, Petrović Z Lj and Makabe T 2000 *J. Vac. Sci. Technol.* A **18** 864
[35] Skullerud H R 1968 *J. Phys. D: Appl. Phys.* **1** 1567
[36] Itoh H and Musha T 1960 *J. Phys. Soc. Japan* **15** 1675
[37] Longo S, Capitelli M, 1993 *Plasma Chem. Plasma Process.* **14** 1
[38] Vasenkov A V 2000 *J. Appl. Phys.* **88** 626
[39] Nollan A M, Brennan M J, Ness K F and Wedding A B 1997 *J. Phys. D: Appl. Phys.* **30** 2865
[40] White R D, Brennan M J and Ness K F 1997 *J. Phys. D: Appl. Phys.* **30** 810
[41] Kumar K, Skullerud H R and Robson R E 1980 *Aust. J. Phys.* **33** 343
[42] Raspopović Z M, Sakadžić S, Bzenić S A and Petrović Z Lj 1999 *IEEE Trans. Plasma Sci.* **27** 1241
[43] Robson R 1991 *Aust. J. Phys.* **50** 577
[44] White R D, Robson R E and Ness K F 1999 *Phys. Rev.* E **60** 7457
[45] Robson R E, White R D and Petrović Z Lj 2005 *Rev. Mod. Phys.* **77** 1304
[46] Shimada T, Nakamura Y, Petrović Z Lj and Makabe T 2003 *J. Phys. D: Appl. Phys.* **36** 1936
[47] Kurihara M, Petrović Z Lj and Makabe T 2000 *J. Phys. D: Appl. Phys.* **33** 2146
[48] Dujko S, White R D, Ness K F, Raspopović Z M, Petrović Z Lj and Robson R E 2004 *Proc. 14th Int. Symp. Electron Molecule Collisions and Swarms* ed S d'A Sanchez *et al* (Campinas, SP, Brazil) p 98
[49] Petrović Z Lj, Crompton R W and Haddad G N 1984 *Aust. J. Phys* **37** 23
[50] Robson R E 1984 *Aust. J. Phys.* **37** 35
[51] Vrhovac S B and Petrović Z Lj 1996 *Phys. Rev.* E **53** 4012
[52] Aleksandrov N L, Dyatko N A, Kochetov I V, Napartovich A P and Lo D 1996 *Phys. Rev.* E **53** 2730
[53] Yamamoto K and Ikuta N 1999 *J. Phys. Soc. Japan* **68** 2602
[54] White R D, Ness K F and Robson R E 1999 *J. Phys. D: Appl. Phys.* **32** 1842
[55] Ness K F and Robson R E 1986 *Phys. Rev.* A **34** 2185